17th World Conference on Earthquake Engineering, 17WCEE
Sendai, Japan - September 13th to 18th 2020

STRUCTURAL PERFORMANCE EVALUATION OF SHEAR-fAILING RC COLUMNS WITH LARGE LONGITUDINAL REINFORCEMENT RATIO

T. Nakamura[(1)], K. Miyajima[(2)], and I. Yamamoto[(3)]

[(1)] *Associate Professor, Niigata University, takaya@eng.niigata-u.ac.jp*
[(2)] *Graduate Student, Niigata University, f18e046b@mail.cc.niigata-u.ac.jp*
[(3)] *Graduate Student, Niigata University, f19e062j@mail.cc.niigata-u.ac.jp*

Abstract

In the structural design of reinforced concrete (RC) buildings, shear-failing columns are avoided because of the risk of brittle failure and loss of axial load carrying capacity. However, the damage behavior of shear-failing RC columns varies with the amount of longitudinal reinforcement. The greater is the amount of longitudinal reinforcement, the larger is the maximum strength and deformation capacity, and the less likely it is to undergo the loss of axial load carrying capacity. Thus far, tests on shear-failing RC columns with large longitudinal reinforcement have not been conducted. Hence, the effect of large longitudinal reinforcement on structural performance of the columns has not been studied. Therefore, in this study, the static loading test of shear-failing RC columns with large amount of longitudinal reinforcement was conducted, and the effect of longitudinal reinforcement on structural performance of the columns, such as the maximum strength, load-degradation after the maximum load, and deformation capacities, was studied. Though the shear-failing RC columns are avoided in structural design, if their maximum strength is large and deformability after the maximum load is high, they can be used effectively for structural design.

Five column specimens were fabricated and designed to ensure shear failure. The column heights and sections (width × depth) were 900 mm and 450 × 450 mm, and 540 mm and 270 × 270 mm; the height-to-depth ratio was 2.0 for all specimens. Normal reinforcement and concrete were used. The transverse reinforcement ratio was 0.53%. Though the specimens were shear-failing columns, a high transverse reinforcement ratio was selected, assuming that they would be used for newly designed buildings. The test variable was the longitudinal reinforcement ratio (p_g), defined as the total main reinforcement area to the column section, which were 1.7%, 3.0%, 4.7%, 6.4%, and 8.3%. Note that the lower limit of the p_g in Japanese seismic code is 0.8%; the p_g for specimens considerably exceeded this limit. However, specimens with high p_g were studied to examine the possibility of use in structural design. The specimens were laterally loaded under constant axial load. The axial stress ratio was approximately 0.2 times the concrete strength, multiplied by the column section. Cyclic loading was used as loading history.

The study revealed that the larger is the p_g, the greater is the maximum strength, lateral drift at maximum strength, ultimate lateral drift, and collapse drift. Note that the ultimate lateral drift was defined as the lateral drift caused, when the lateral load decreased by 80% of the maximum strength and was used to evaluate the deformability of columns. Regarding maximum strength, the observed values agreed with the computed ones that were calculated using an existing empirical equation, commonly used in Japan. These results indicated the possibility to accept shear-failing RC columns in structural design, if the p_g was sufficiently large.

Keywords: Reinforced concrete column, Shear failure, Longitudinal reinforcement ratio, Collapse

1. Introduction

In the structural design of reinforced concrete (RC) buildings, shear-failing columns are avoided because of the risk of brittle failure and collapse, which is defined as the loss of axial load carrying capacity. However, the damage behavior of shear-failing RC columns varies with the amount of longitudinal reinforcement. An increased longitudinal reinforcement results in larger maximum strength values and deformation capacity, thus, reducing the possibility of collapse of a structure. Tests on shear-failing RC columns with large longitudinal reinforcement have not been conducted till present. Hence, the effect of large longitudinal reinforcement on the structural performance of the columns has not been studied. This, therefore, is a novel study involving the application of a static loading test on shear-failing RC columns with a large amount of longitudinal reinforcement. The effect of longitudinal reinforcement on structural properties of the columns, such as the maximum strength, load degradation after the maximum load, and deformation capacity, was determined. The collapse process of RC columns was also studied. Although the use of shear-failing RC columns is avoided in structural design, they can be used effectively if their maximum strength is high and if they maintain a high deformability after the maximum load.

2. Outline of test

2.1 Specimen

Five column specimens were fabricated and designed to ensure shear failure. Table 1 lists the structural properties of the specimens. Two Series (Series 1 and 2) were considered. As examples, the reinforcement details and the column sections of the specimens PG1.7 (Series 1) and PG4.7 (Series 2) are shown in Fig. 1.

All the five specimens had the same measurement values: the height-to-depth ratio h_0/D was 2.0; the transverse reinforcement ratio p_w was 0.53%; and the axial stress ratio η was approximately 0.2. Though the specimens were shear-failing columns, a high p_w was selected, assuming that they would be used for newly designed buildings.

The test variable was the longitudinal reinforcement ratio p_g, defined as the total main reinforcement area to the column section, which were 1.7%, 3.0%, 4.7%, 6.4%, and 8.3%. Note that the lower limit of the p_g in Japanese seismic code is 0.8%; the p_g for specimens considerably exceeded this limit. However, specimens with high p_g were studied to examine the possibility of use in structural design. We conducted the test on columns having these p_g values and obtained novel results regarding the structural performance of RC columns with large longitudinal reinforcements.

Table 1 – Structural properties of specimens

Name [1]	Series	Width×depth b × D (mm × mm)	Height h_0 (mm)	h_0/D	Transverse reinforcement ratio p_w (%)	Axial stress ratio η [2]	Longitudinal reinforcement ratio p_g [3] (%)
PG1.7	Series 1	450 × 450	900	2.0	0.53 (2-D10@60)	0.18	1.7 (12-D19)
PG3.0							3.0 (12-D25)
PG4.7	Series 2	270 × 270	540	2.0	0.53 (2-D6@45)	0.19	4.7 (12-D19)
PG6.4							6.4 (12-D22)
PG8.3							8.3 (12-D25)

(1) The Number after PG in each specimen denotes the longitudinal reinforcement ratio in percentage; (2) axial stress ratio, $\eta = N / (b \cdot D \cdot \sigma_B)$, where N: axial load; (3) the Number after D denotes the bar diameter in mm.

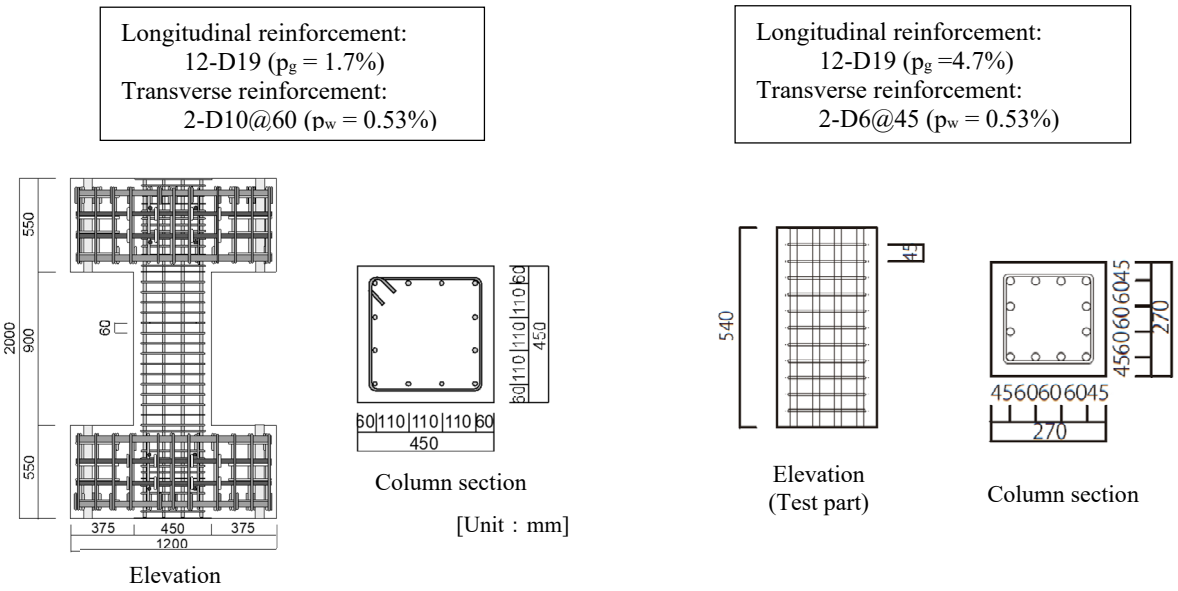

Fig. 1 – Reinforcement details

Table 2 presents the material properties. Normal reinforcement and concrete were used.

Table 3 lists the shear and flexure strengths computed for each specimen by the conventional equation in Japan [1].

Table 2 – Material properties

(a) Series 1

Steel				Concrete
		Yield stress (N/mm^2)	Strain at yield stress (%)	Max. stress σ_B (N/mm^2)
Longitudinal reinforcement	D19	383	0.25	25.0
	D25	383	0.25	
Transverse reinforcement	D10	399	0.25	

(b) Series 2

Steel				Concrete
		Yield stress (N/mm^2)	Strain at yield stress (%)	Max. stress σ_B (N/mm^2)
Longitudinal reinforcement	D19	407	0.26	31.4
	D22	388	0.23	
	D25	383	0.25	
Transverse reinforcement	D6	424	0.36	

Table 3 – Computed strength

Name	Series	Shear strength (1) (kN)	Flexure strength (kN)	Shear/Flexure
PG1.7	Series 1	514	750	0.69
PG3.0		549	1038	0.53
PG4.7	Series 2	222	535	0.41
PG6.4		229	652	0.35
PG8.3		237	806	0.30

(1) calculated using the Arakawa minimum formula

2.2 Loading method

The specimens were laterally loaded under constant axial load. For the test apparatus, a pantograph was used to prevent the loading beam on the column top from rotating and realizing double-curvature deformation.

With respect to the loading history, we used cyclic loading conditions. Fig. 2 shows the detailed loading history: the lateral drifts were divided by the column height. The specimens were finally loaded to the positive direction. Loading for Series 1 specimens continued until the specimens lost their axial load-carrying capacity, i.e., they collapsed.

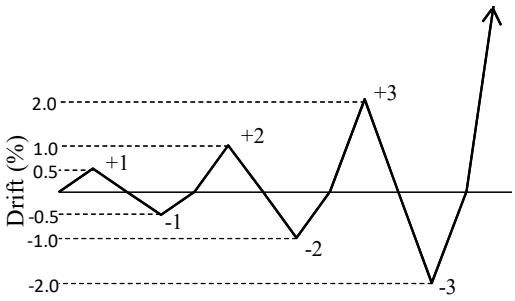

Fig. 2 – Loading history

3. Test results of Series 1 specimens

3.1 Collapse procedure

The specimens of Series 1 experienced shear failure before flexural yielding and finally lost their axial load-carrying capacity. In this study, “collapse” was defined as the column’s loss of axial load-carrying capacity. Fig.3 shows the lateral load, lateral drift relations and damage states observed after the collapse for specimens PG1.7 and PG3.0. The drifts were divided by the column height. In Fig. 3, each square, triangle, and circle indicates the maximum load, ultimate drift, and collapse drift, respectively. In this study, “ultimate drift” was defined as the drift when the load decreased to 80% of the maximum load. The ultimate drift was used to evaluate the plastic deformability of columns before sustaining a certain level of lateral load. Furthermore, “collapse drift” was defined as the maximum lateral drift experienced prior to the collapse. The collapse drift was discussed to evaluate the final deformability of columns. The collapse procedures for PG1.7 and PG3.0 are described below.

For specimen PG1.7, the maximum strength and the associated drift were 637 kN and 0.69%, respectively. Consequently, a wide shear crack developed. The ultimate and collapse drifts were 1.2% and 7.7%, respectively. As shown in Fig. 3, the specimens collapsed when the lateral load decreased to

approximately zero. At the time of collapse, fractures at the transverse reinforcements, loosening at the hook, and buckling of the longitudinal reinforcements were observed. A similar behavior was observed at the time of the collapse of specimen PG3.0.

For specimen PG3.0, maximum strength and associated drift were 750 kN and 0.89%, respectively. The ultimate and collapse drifts were 1.5% and 17.1%, respectively.

The maximum strengths and the ultimate drifts will be discussed later in Chapter 5.

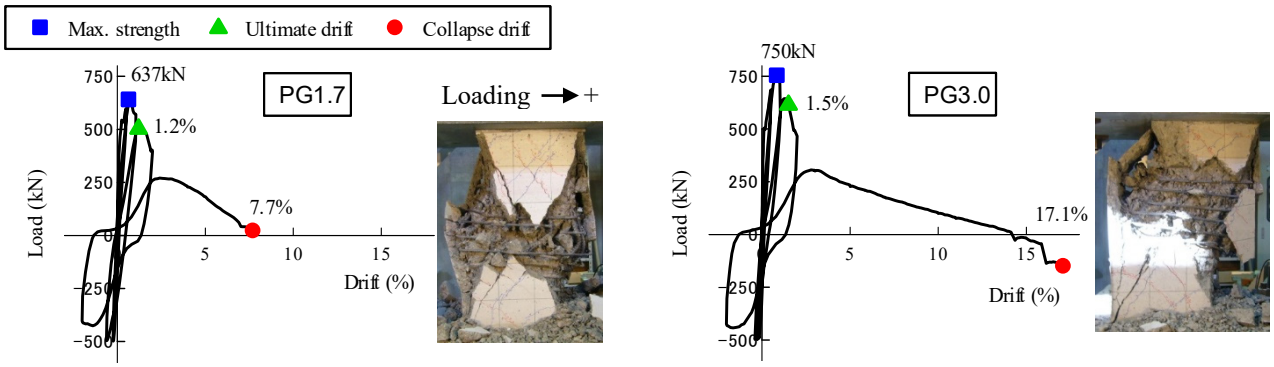

Fig. 3 – Lateral load vs. lateral drift and damage states observed after collapse for specimens of Series 1

3.2 Effect of longitudinal reinforcement ratio on the collapse drift

As stated earlier, the collapse drift of specimen PG1.7 was 7.7% and that of specimen PG3.0 was 17.1%. The latter with the larger longitudinal reinforcement ratio was 2.2 times larger than the former.

Fig. 4 shows the longitudinal reinforcement ratio versus collapse drift relations for specimens PG1.7 and PG3.0 and the test results of existing research [2, 3]. Test variables of the past tests were as follows. The longitudinal reinforcement ratios were 1.7% and 2.7%, the transverse reinforcement ratios were 0.11% and 0.21%, the axial stress ratios were 0.19 and 0.2, and the height-to-depth ratios h_0/D were 2.0 and 3.0, respectively. Normal reinforcement and concrete were used for all specimens. All specimens failed in shear mode before undergoing flexural yielding. In Fig. 4, two specimens that only differed in the longitudinal reinforcement ratio are connected by a solid line. According to Fig. 4, increased longitudinal reinforcement ratios correspond to larger collapse drift values. It means that if the longitudinal reinforcement ratio was larger, the columns could also sustain the axial load for larger drifts without collapsing.

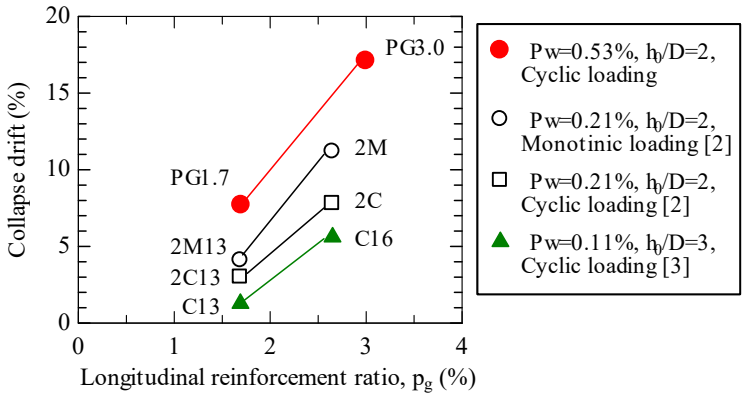

Fig. 4 – Longitudinal reinforcement ratio vs. collapse drift

4. Test results of Series 2 specimens

4.1 Damage procedure

Series 2 failed in shear before flexural yielding. The tests for Series 2 were terminated before the specimens collapsed because the test apparatus was limited and could not accommodate higher lateral drift. Fig. 5 shows the lateral load and the lateral drift relations. In Fig. 5, each square and triangle indicates the maximum load and ultimate drift, respectively. The maximum strengths and the ultimate drifts will be discussed in Chapter 5.

Fig. 6 shows the damage states observed when the drift increased and reached 7%. The reason that we focused on the drift at 7% was to investigate the axial deformation performance within the large drift region. According to Fig. 6, the shear crack width of specimen PG8.3 was the smallest. Thus, larger p_g values lead to reduced crack width and damage in RC columns.

Fig.7 compares the lateral drift and the axial deformation relations of specimens PG4.7 and PG8.3. The axial deformations were divided by the column height. As shown in Fig. 7, the axial deformations increased as the lateral drift increased in the large deformation area. At a drift of 7%, the axial deformation of specimen PG4.7 was 0.49% while that of specimen PG8.3 was 0.22%. The latter with the largest longitudinal reinforcement ratio experienced a deformation 0.45 times less than the former. Therefore, a larger longitudinal reinforcement ratio, corresponds to smaller axial deformation.

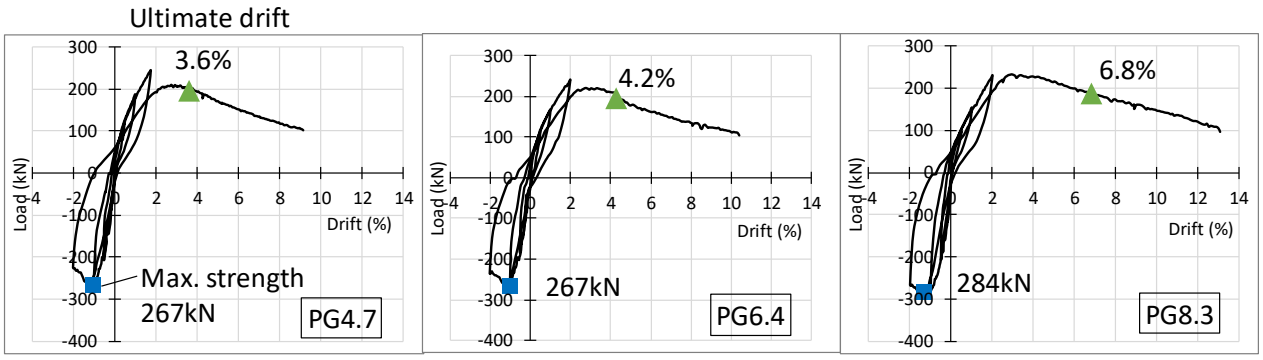

Fig. 5 – Lateral load vs. lateral drift for specimens of Series 2

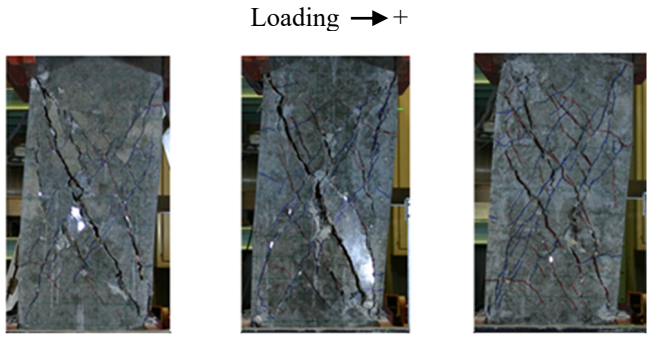

	PG4.7	PG6.4	PG8.3
Axial deformation	0.49%	0.36%	0.22%

Fig. 6 – Damage states at a lateral drift of 7% for specimens in Series 2

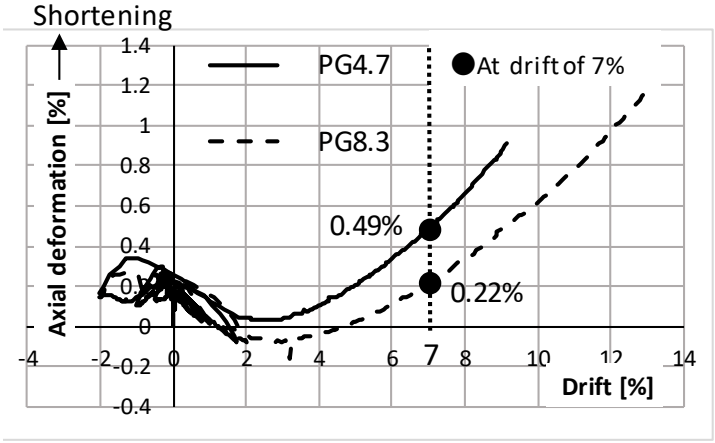

Fig. 7 – Lateral drift vs. axial deformation for specimens in Series 2

4.2 Strain of longitudinal reinforcement

In this section, the longitudinal reinforcement behavior of specimens is discussed based on their strain measurements. The strain gauge locations of longitudinal reinforcement and the longitudinal reinforcement strains of the strain gauge for specimens PG4.7, PG6.4, and PG8.3 are shown in Fig. 8 and Fig. 9, respectively. As shown in Fig. 9, the longitudinal reinforcement strains increased as the lateral drift increased in the large deformation area. Larger longitudinal reinforcement ratios are correlated with smaller longitudinal reinforcement strains. The gauge location was close to the shear crack (Fig. 6), indicating that concrete crushing near the failure line led to the increase in compression strain in the longitudinal reinforcements [4]. According to Fig. 9, the longitudinal reinforcement strains of the three specimens had not reached their yield strains (see Table 2). Thus, it can be assumed that the specimens with the large longitudinal reinforcement ratios were still resistant to collapsing.

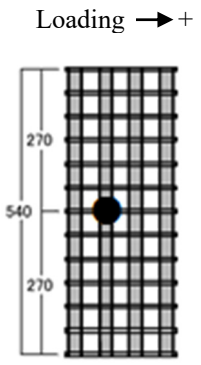

[Unit: mm]

Fig. 8 – Strain gauge location

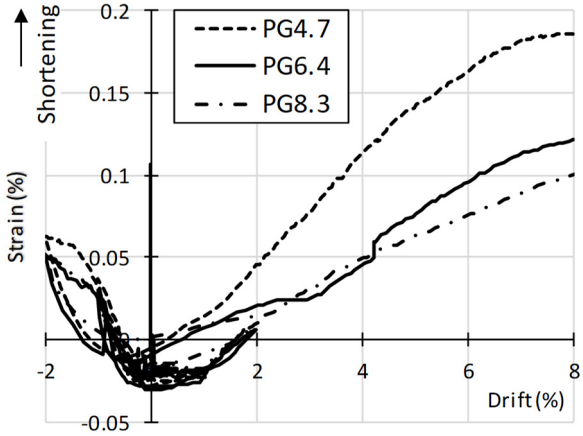

Fig. 9 – Drift vs. longitudinal reinforcement strain

5. Discussion

The test results of Series 1 and 2 are presented in Table 4. Effects of longitudinal reinforcement ratio on such results are discussed below.

Table 4 – Test results

Name	Series	Maximum strength (kN)	Drift at maximum strength (kN)	Ultimate drift (%)	Axial deformation at drift of 7% (%)	Collapse drift (%)
PG1.7	Series 1	637	0.7	1.2	1.0	7.7
PG3.0		750	0.9	1.5	0.67	17.1
PG4.7	Series 2	267	1.0	3.6	0.49	—
PG6.4		267	1.0	4.2	0.36	—
PG8.3		284	1.4	6.8	0.22	—

5.1 Maximum strength

Fig. 10 shows the longitudinal reinforcement ratio, p_g, versus maximum strength relations for the specimens of Series 1 and 2. The maximum strengths were converted to maximum shear stresses using Eq. (1). This is because the cross-sectional areas of the specimens of Series 1 and 2 were different.

$$\tau = Q / (b \times j) \quad (1)$$

where τ is the shear stress, b is the column width, and j is the distance between the resultant values of tension and compression (j = (7/8) d, where d is the effective depth).

According to Fig. 10, the maximum shear stress of specimen PG1.7, which has the smallest p_g was 4.1 N/mm^2 and that of specimen PG8.3, which has the largest p_g, was 5.3 N/mm^2. The latter is 1.3 times stronger than the former. Thus, a higher p_g corresponds to a higher maximum strength.

Fig. 10 also shows the maximum shear strength computed using the Arakawa mean equation which is commonly used in Japan [1]. The values in parentheses are the ratios of the tested maximum strengths to the computed values. The experimental values were higher than the calculated values for all specimens. For Series 2, the experimental and calculated values are close. Thus, the experimental values of maximum strength can be evaluated using the calculated values.

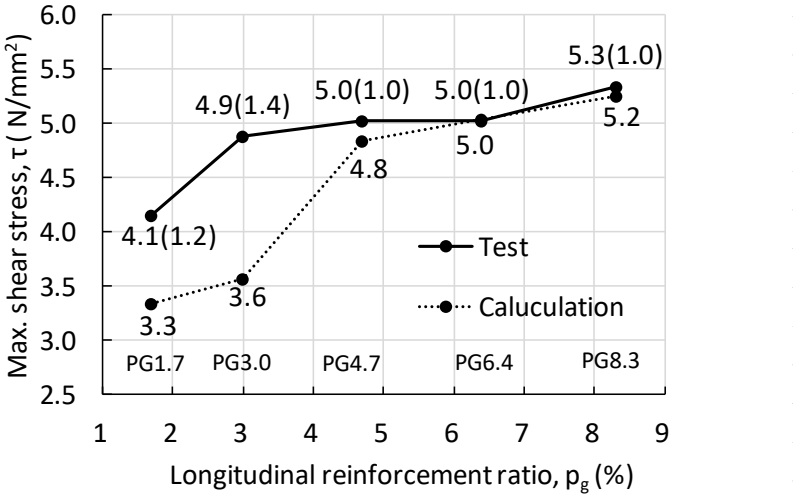

Fig. 10 – Longitudinal reinforcement ratio vs. maximum strength

5.2 Drift at maximum strength

Fig. 11 shows longitudinal reinforcement ratio, p_g, versus drift at maximum strength relations for the specimens of Series 1 and 2. The drift at the maximum strength of specimen PG1.7 was 0.7% and that of specimen PG8.3 was 1.4%. The latter was 2.0 times larger than the former. Therefore, larger p_g values also correspond to larger drift values at the maximum strength.

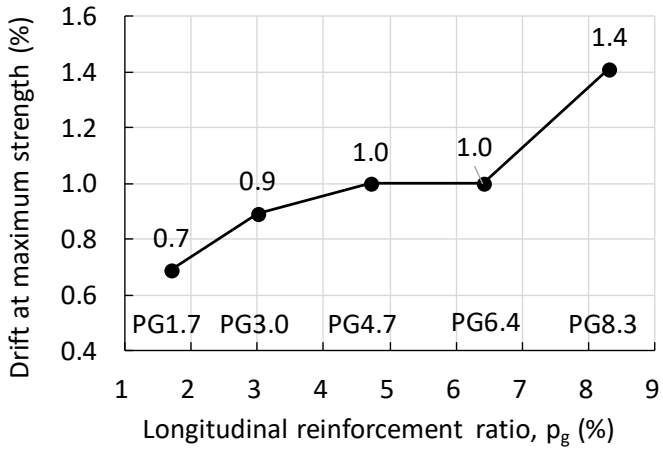

Fig. 11 – Longitudinal reinforcement ratio vs. drift at maximum strength

5.3 Ultimate drift

As stated before, the ultimate drift was defined as the drift when the load decreased to 80% of the maximum load. In this study, the maximum load and the drift values along the positive direction are considered. Fig. 12 shows longitudinal reinforcement ratio, p_g, versus ultimate drift relations for the specimens of Series 1 and 2. As shown in Fig. 12, the ultimate drift of specimen PG1.7 was 1.2% and that of specimen PG8.3 was 6.8%. The latter exhibited a drift that was 5.7 times higher than the former. The higher p_g values correspond to higher

ultimate drift values. Thus, the plastic deformability of shear-failing RC columns after the maximum load is greater at high p_g.

The ultimate drift is analogous to the inter-story drift of a real-scale building with particular geometric properties. The assumed geometric properties are shown in Fig. 13. For Series 2, the columns, which are 2.5 times larger than the specimens in size, are assumed to behave in the same way as the specimens did. The inter-story ultimate drift (%) of this building, at which the ultimate drift occurs, is computed by multiplying the ultimate drift (%) of the specimens by a factor of 1350 / 3600 = 0.375 which is the ratio of the column clear height of 1350 mm and the story height of 3600 mm. For series 1, the inter-story ultimate drift is 0.25 times the ultimate drift. The computed ultimate inter-story drift values are shown in Fig. 12 and denoted by the numbers in parentheses. An upper limit of maximum inter-story drift during earthquakes is 1/200 (= 0.5%) for the allowable stress design method in Japanese building code. According to Fig. 13, the inter-story ultimate drifts of PG1.7 and PG3.0 are lower than the limit. This means that building using those longitudinal reinforcement ratios could exhibit a maximum inter-story drift which exceeds the limit during a severe earthquake, hence, making them unacceptable. On the other hand, the inter-story ultimate drifts of PG4.7, PG6.4, and PG8.3 are larger than the limit. This means that, in a similar earthquake, the maximum inter-story drift of building with these ratios might be smaller than the prescribed limit in the code. the safety margin increases as the longitudinal reinforcement ratio increases.

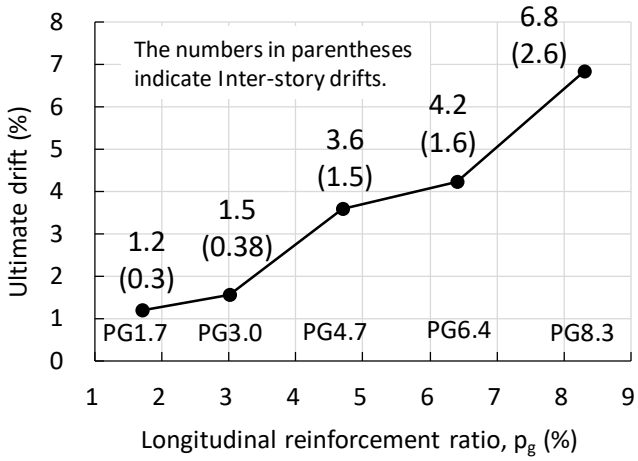

Fig. 12 – Longitudinal reinforcement ratio vs. ultimate drift

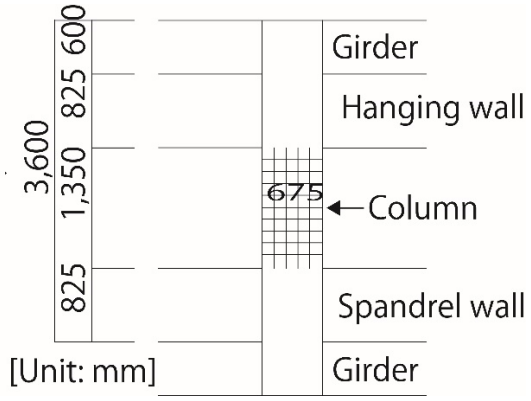

Fig. 13 –Assumed real-scale building (Series 2)

5.4 Axial deformation at a drift of 7%

Fig. 14 shows longitudinal reinforcement ratio, p_g, versus axial deformation at a lateral drift of 7% for specimens of Series 1 and 2. As stated earlier, the reason we that focused on the drift at 7% was to investigate the axial deformation performance within the large drift region. As shown in Fig. 14, the axial deformation of specimen PG1.7 is 1.0% and that of specimen PG8.3 is 0.22%. The latter is 0.2 times less than the former. A higher p_g, therefore, corresponds to a lower axial deformation at a drift of 7%. Within the large drift region, columns with higher p_g resist shortening better.

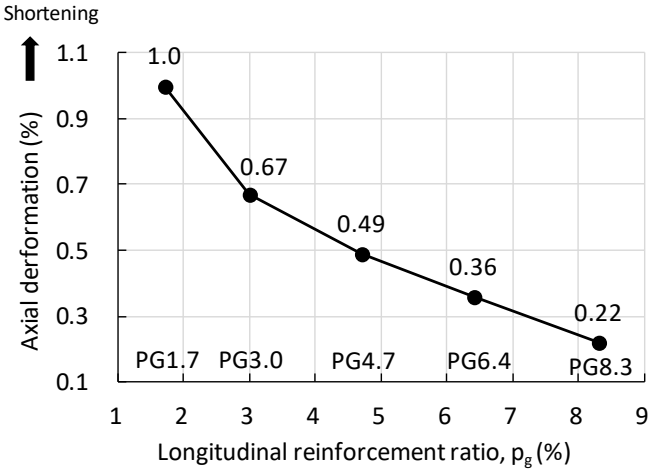

Fig. 14 – Longitudinal reinforcement ratio vs. axial deformation at a drift of 7%

6. Conclusions

The effects of longitudinal reinforcement ratio, p_g, on the damage behavior of shear-failing RC columns were determined using a static loading test. The p_g values ranged from 1.7% to 8.3%. The major findings of this study are summarized below:

1) A higher p_g value is correlated with larger collapse drifts. Columns with higher p_g can sustain axial loads for larger drifts without collapsing.

2) A higher p_g value is correlated with higher maximum strength. The maximum shear stress of the column with p_g of 8.3% was 1.3 times higher than that of the column with p_g of 1.7%. The associated drift at the maximum strength is also positively correlated with p_g.

3) A higher p_g value is correlated with larger ultimate drift, which was defined as the lateral drift when the lateral load decreased to 80% of the maximum load. Thus, the plastic deformability of RC columns after the maximum load increases as p_g increases.

4) Columns with higher p_g experience less axial deformation in the large deformation region.

5) A higher p_g results in shorter longitudinal reinforcement strain and smaller shear crack width in the large deformation region.

We conclude that the shear-failing RC columns with higher p_g possess higher maximum strength and improved plastic deformability in the large deformation area. These results favor the use of shear-failing RC columns in structural design, provided that the longitudinal reinforcement ratio is sufficiently large.

7. Acknowledgements

The authors express their gratitude to Mr. K. Ito and Ms. Y. Mizuno, former students of Niigata University, for their assistance.

This work was supported by JSPS Grants-in-Aid for Scientific Research Grant: Number 17K06636 and Collaborative Research Projects (CRP)- 2019: Laboratory for Materials and Structures, Institute of Innovative Research, Tokyo Institute of Technology.

8. References

[1] Ministry of Land, Infrastructure, Transport and Tourism et al. (2016) “Commentary on Structural Regulations of the Building Standard Law of Japan” (in Japanese)

[2] Takaya N and Manabu Y (2003) “Axial Collapse of R/C Short Columns”, Proceedings of fib Symposium -Concrete Structures in Seismic Regions-, Paper No. 159

[3] Hongri J, Manabu Y and Takaya N (2005) “Effect of Transverse Walls on Collapse of RC Columns with Shear Mode”, Proceedings of the Japan Concrete Institute, Vol. 27, No. 2, pp. 193-198 (in Japanese)

[4] Manabu Y (2008) “Formulation of Post-Peak Behavior of Old Reinforced Concrete Columns Until Collapse”, Proceedings of the Fourteenth WCEE, Paper ID:05-03-0104, 2008

